Available online at www.sciencedirect.com
SCIENCE DIRECT®
International Journal of Thermal Sciences 45 (2006) 310–320
International Journal of Thermal Sciences
www.elsevier.com/locate/ijts

High speed video recording of bubble formation with pool boiling

Andrea Luke [a,*], Da-Chuan Cheng [b]

[a] *Institut für Thermodynamik, Universität Hannover, Callinstr. 36, 30167 Hannover, Germany*
[b] *Institute of Pattern Recognition and Image Processing, Department of Computer Science, Albert-Ludwigs-Universität Freiburg, 79110 Freiburg, Germany*

Received 21 October 2004; received in revised form 15 May 2005; accepted 2 June 2005

Available online 7 November 2005

Abstract

A general theory for boiling heat transfer shall be developed by modelling the microscopic transport phenomena in boiling on a heated surface supported by experimental studies with equally detailed informations on roughness, formation of bubbles and on heat transfer. The heat transfer measurements and the bubble formation are carried out during the same experiment. The experiments in bubble formation are obtained by a high speed video technique.

The images of the video sequence are analysed manually or by special semiautomatic evaluation programs to obtain the number and location of active nucleation sites and some selected results for bubble departure diameter and frequency. Results for the bubble formation on a horizontal copper tube in boiling propane for an intermediate pressure from low to high heat fluxes are discussed, e.g. the cumulative site densities vary from 2 mm^{-2} at low heat fluxes to 70 mm^{-2} for high heat fluxes. Additionally, the fluctuation by time and in the location on the tube is recorded. Because of the large amount of data, different automatic methods to analyse the single images have to be developed. A new template-based method for the evaluation of the video sequences allows the nearly automatic identification of the individual bubble on its nucleation site, and to track its growth and movement along the heated tube surface during the following images. First results show that the bubbles sliding up the superheated tube surface grow at a similar rate as those staying on their nucleation site. Their contribution for the vapour production in model assumptions has to be revised.

Keywords: Pool boiling; Nucleation sites; Bubble formation; Bubble growth; Video sequence analysis

1. Introduction

High heat flux densities can be transferred by small temperature gradients in evaporators. The high transfer capability becomes important even in fields like electronic facilities, where two-phase systems have been avoided until now for reasons of their complexity. The efforts to a better understanding of the fundamental processes in boiling heat transfer will increase in future as evaporators are more and more miniaturized in different operative ranges to save costs and energy and to preserve the natural resources. This trend is supported by new developments in computer calculations and in measurement techniques.

The calculation methods for the design of evaporators are based on more or less accurate heat transfer measurements [1]. They are often not attended by equally accurate studies of the roughness of the heated surface and of the bubble formation. The characteristic features of the heating surface and of the bubble formation are not introduced into the usual empirical predictive methods [2]. The joint research project on fundamentals of boiling heat transfer aims at a better modelling of the basic heat transfer phenomena by activation of the bubbles, the vapour movements on the heated surface and their consequences on the integral heat transfer. The final idea is to develop calculation methods for the design of evaporators of high efficiency considering more the physical phenomena than the empirical methods [1,2] used now. Therefore, the roughness of the heated surfaces [3], the heat transfer and bubble formation [4,5] or vapour production [6], respectively, are investigated by experiment and theory [7].

The formation and the growth of bubbles in their favoured sites on the heated surface is one of the essential mechanisms in boiling heat transfer by which the local superheat in the liq-

* Corresponding author. Tel.: +49 0511 762 2277; fax: +49 0511 762 3857.
E-mail addresses: luke@ift.uni-hannover.de (A. Luke), cheng@informatik.uni-freiburg.de (D.-C. Cheng).

1290-0729/$ – see front matter
doi:10.1016/j.ijthermalsci.2005.06.011

Nomenclature

A	area	m^2
d	bubble diameter	mm
D	tube diameter	m
g	density distribution	
Δh_v	heat of vaporization	$J \cdot kg^{-1}$
h	probability function	
m	exponent	
N	number of active nucleation sites	
(N/A)	number of active nucleation sites per heated area	mm^{-2}
p	pressure	Pa, bar
p^*	reduced pressure, $= p_s/p_c$	
p_c	critical pressure	Pa , bar
p_s	saturation pressure	Pa, bar
P_a	standardized roughness parameter according to DIN EN ISO 4287	µm
q	heat flux	$W \cdot m^{-2}$
r_c	critical radius of stable bubble nuclei	m
s_{act}	nearest distance between neighbouring cumulative nucleation sites	mm
T	temperature	K
ΔT	superheat	K

Greek symbols

α	heat transfer coefficient	$W \cdot m^{-2} \cdot K^{-1}$
ρ'	density of the saturated liquid	$kg \cdot m^{-3}$
ρ''	density of the saturated vapour	$kg \cdot m^{-3}$
σ	standard deviation	
σ	surface tension	$N \cdot m^{-1}$
φ	azimuthal angle	°

Subscripts

A	departure
B	bubble
c	critical
cum	cumulative
m	mean
s	saturated
sim	simultaneous
w	wall

uid and in the wall is reduced. The turbulences of the growing, departing and up-sliding bubbles cause good heat transfer along the heated surface and within the evaporator. The interaction of the properties of the heated surface (e.g. material, microstructure and macrostructure, geometry, wettability of the surface by the liquid) and of the boiling liquid, and the operating parameters result in a number of influence parameters on bubble formation and heat transfer.

New high speed video technique offers the possibility to get more detailed information of the bubble formation on the heated surface in situ. The activation, growth and movement after the departure of the individual bubbles are observed and digitally recorded. The experimental data can be evaluated quantitatively by means of special semi-automatic evaluation methods of the images of the high speed video sequences. Selected recently published results of the bubble formation evaluated by this methods are discussed for intermediate pressures from low to high heat fluxes of boiling propane on an horizontal copper tube with a fine sandblasted surface (average mean roughness $P_a = 0.25$ µm [3]; cf. [8] for the heat transfer results in detail). New automatically evaluating methods have to be developed because of the large quantity of data within the image sequences [9]. The method is applied to individual bubbles growing on their nucleation sites and they are tracked on their way sliding up the superheated boundary layer around the tube. First results of the new evaluation method are presented within this paper.

2. Evaluation of the high speed video sequences

A number of experimental set-ups used in the past, were limited to atmospheric conditions [4]. Therefore, the standard apparatus had been established by Gorenflo for pool boiling experiments suited for a large range of temperature and pressure (for details see for instance [4] in this issue and e.g. [10]). The main features of the apparatus are

- the dc-heated horizontal test tube in the evaporator,
- evaporator and condenser combined in a natural circulation loop for the test fluid and placed in a conditioned chamber of which the air temperature is adjusted to the saturation temperature T_s of the liquid in the evaporator.

The microstructure and macrostructure of the heated surface are analysed in advance of the heat transfer measurements by a three-dimensional contactless roughness measurement technique combining the stylus technique with near field acoustic microscopy [3].

2.1. Review of evaluation methods for bubble formation in literature

Most of the model assumptions for bubble formation in pool boiling are based on the observation of noninfluenced single bubbles. Nevertheless, it is obvious that these assumptions are only valid for very low heat fluxes or superheat and for horizontal, plane heated surfaces. On tubes or on vertical plates, the bubbles are already influenced from the instant of beginning nucleation. A connection between the measured heat transfer and the parameters of bubble formation is important for the validation of model assumptions like those of Genske and Stephan [7,11] and Kern and Stephan [12]. The parameters of bubble formation are the bubble departure diameter and frequency, the number of active nucleation sites and their local distribution on the surface, the growth of the bubbles at their nucleation sites

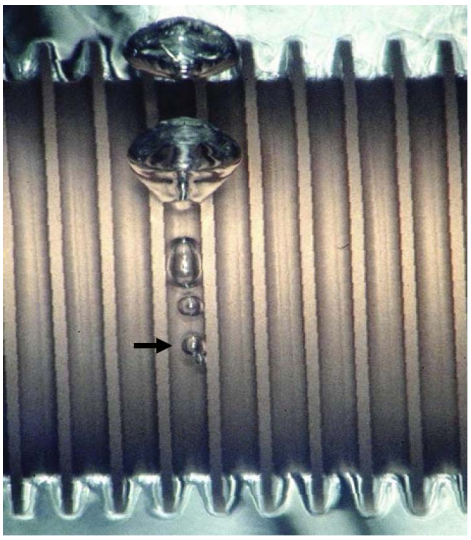

Fig. 1. Photograph of boiling n-hexane on a horizontal fine sandblasted finned tube ($p^* = 0.037$, $q = 3.4$ kW·m^{-2}). Determination of the bubble departure diameter, see the arrow from [14].

and during their path sliding up near the superheated boundary layer.

The main aim is to develop noninvasive methods for the investigation of bubble formation to avoid the disturbance of the boiling process. The methods proposed in literature are

- photographs [13,14];
- high speed video technique [15–17];
- holography [18];
- combination of temperature measurements by liquid crystals with high speed video technique [19];
- optical and electrical probes for the evaluation of the distribution of vapour/liquid interphase combined with the measurement by micro thermocouples [6];
- tomography [20];
- counting of deposits or little holes on the surface evoked by nucleation sites [21].

In general, photographs give a qualitative impression of the bubble formation, e.g. the influence of the operating parameters as saturation pressure and heat flux. Nevertheless, a lot of quantitative measurements result from the evaluation of photographs cf., e.g. [22], especially for low heat fluxes and pressures, e.g. the bubble departure diameter is defined as the second bubble within a chain of bubbles, see the arrow in Fig. 1 [14]. The main problem of this method is the missing temporal resolution. The moment of departure cannot be fixed exactly and the separation of bubbles sliding up the tube surface from those still growing on their nucleation sites is difficult. This explains the large scatter of these data in the literature.

High speed video technique now offers the possibility to get more detailed and higher temporally resolved information of the bubbles and their activation on the heated surface. Therefore, the bubble formation is examined in parallel to the heat transfer measurements on the one hand by photographs and on the other by high speed video technique with a temporal resolution of 1000 images·s^{-1}. Each image consists of 512×512 pixel (Company Weinberger, Karlsruhe, Germany). The observation time, i.e. the length of one video sequence, is 500 ms (= 500 images) to reduce the data amount and with regard to the storage capacity of the computer. The video sequences are taken through a sight-glass of the standard apparatus. The bubble formation is recorded successively on different parts of the tube because different illumination set-ups have to be provided [9]. Different sessions of videos are preserved depending on the operation conditions (heat flux, saturation pressure), on the geometry, the microstructure and macrostructure of the tube, and on the boiling liquid (e.g. an area of 5 mm^2 is observed for $p^* = 0.1$ ($p_s = 4.2$ bar) and $q = 20$ kW·m^{-2} in boiling propane to determine active nucleation sites). For higher pressures the area has to be reduced by changing the optical lenses in front of the camera in order to separate the individual sites from each other [23].

The number of active sites have been counted on the area examined and presented true to scale in Fig. 2 by two typical examples of the bubble formation within ca. 4.5×4.5 mm^2 of the test tube surface near the horizontal median line of the copper tube (propane, fine sandblasted surface, $D = 25.4$ mm). Fig. 2 represents two succeeding video images with nucleation sites simultaneously active during 1 ms, indicated by horizontal arrows in Fig. 2, left and right (in the following termed as "simultaneous sites", in former publications designated as "momentaneous sites" [8,15,23]). The number of simultaneously active nucleation sites varies from ms to ms, shown here by two new dashed (angular) arrows in Fig. 2, on the right. The active sites are defined by the existence of new bubbles. These sites have been activated obviously within the time interior between the two images. This demonstrates that the active nucleation sites cannot be found in one single image by itself (or e.g. in a single photograph); instead each of the more than 500 images of a video sequence is analysed by looking forwards and backwards to check the active sites in one ms. The departure moment is the end of activity on the site and is defined by the onset of variation of the local position of the bubble. The sliding bubbles vary their local position quite evidently during 1 ms so a separation from the active sites is possible.

The other visible bubbles on the images in Fig. 2 that have not been marked by arrows are sliding up along the tube surface. The average number of the simultaneous sites within this video sequence is approx. $(N/A)_{\text{sim}} = 9$ mm^{-2} during the total session of 500 ms. As shown in [27] (see also below), the number of the simultaneous nucleation sites are varying largely; this leads to the requirement of the evaluation of each image of the video sequence and not only of a random test of three or five single images as done in former analyses e.g. [23].

Much larger numbers of more than 600 sites (on an area of 4.5 mm × 4.5 mm) are active at least once during the entire 500 ms sequence. They are localized in the diagram in Fig. 3. This "cumulative" site density $(N/A)_{\text{cum}}$ is the total number of sites per unit area being active during some time within the observation time period which has to be much longer than the average growth period of a bubble on its site. Related to the area investigated, this corresponds to a cumulative site density

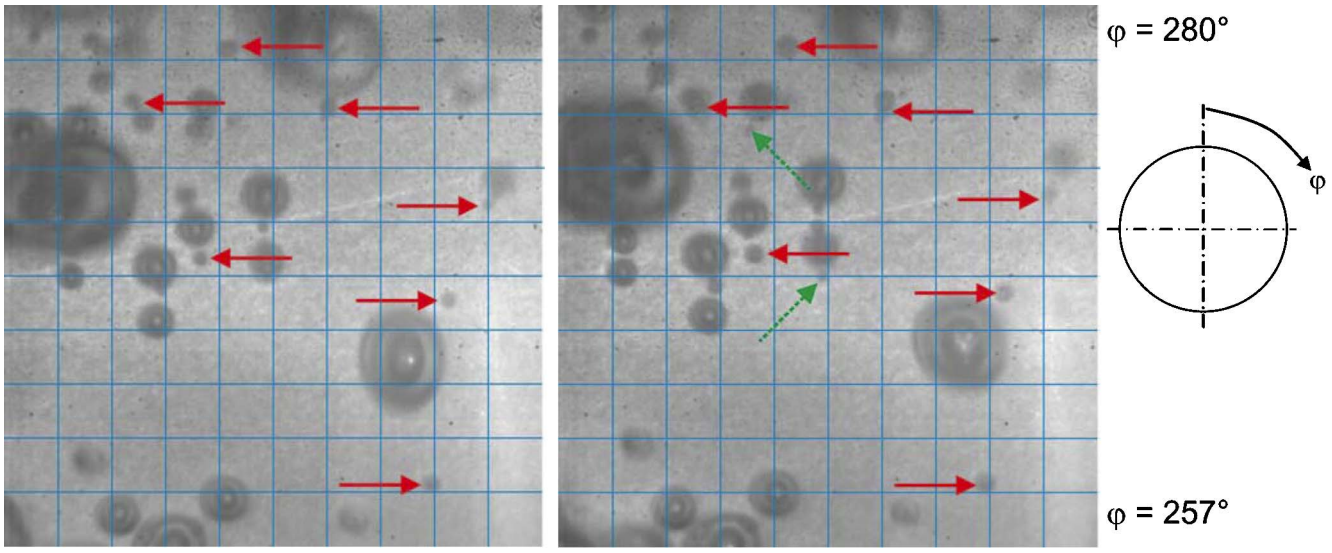

Fig. 2. Bubble formation near the median line of the test tube for propane boiling at $p^* = 0.1$, $q = 20$ kW·m^{-2} (area investigated ca. 4.5 × 4.5 mm): Selected images with typical simultaneous active nucleation sites (horizontal arrows on both images) and activated one ms late (dashed arrows, image on the right).

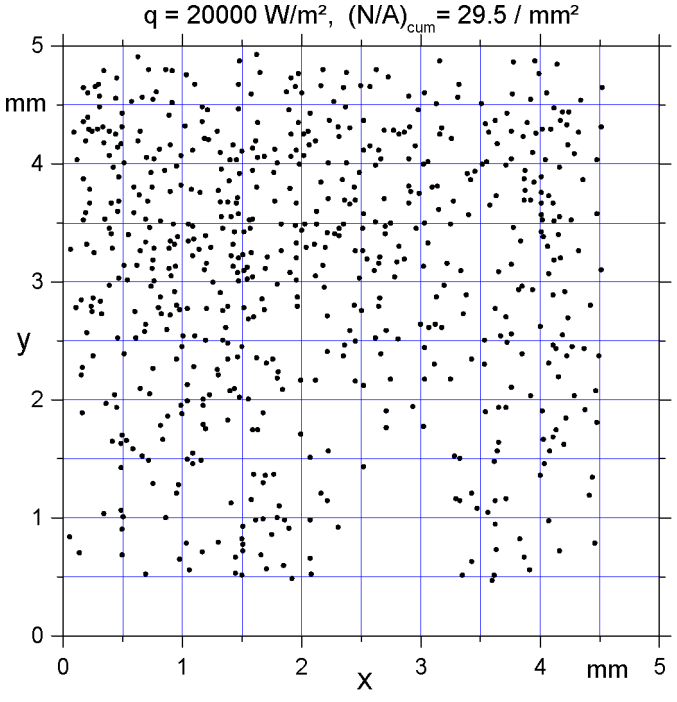

Fig. 3. Local distribution of all active cumulative nucleation sites for propane boiling on an horizontal copper tube at $p^* = 0.1$, $q = 20$ kW·m^{-2} ($D = 25.4$ mm).

of $(N/A)_{\text{cum}} \approx 30$ mm^{-2} in the case of Fig. 3. That means that the simultaneous and cumulative site densities may differ a lot for the same boundary conditions, compare Figs. 2 and 3. For fine sandblasted surfaces, most of the nucleation sites are activated only once during the entire sequence of 500 ms [15]. Following these results, it is essential to mention the observation time (500 ms) and the temporal resolution of the system (1 ms) for the comparison of number of simultaneous or cumulative nucleation sites with data of literature, cf. also [4,5,24]. In consequence, the model assumption of stable nucleation sites with constant frequency and constant departure diameter has to be checked by new data considering the various influence parameters. Additionally, the contribution of sliding bubbles, e.g. their growth and velocity, has to be investigated. The essential large amount of data cannot be evaluated manually, automatic methods are required.

2.2. New method for the evaluation of video sequences

In the past, the evaluation of these videos has been performed by special semi-automatic programs, cf. [4,15,28], that allowed the quantitative determination of various parameters, but were very time consuming because the permanent input of the user was needed (i.e. the analyse of each bubble and each nucleation site in each image of a sequence). In the following, an automatic method for the evaluation of the video sequences is developed therefore, especially concerning the growth and movement of the individual bubble during the recorded observation time [16,25]. A first program allowed the automatic recognition of the bubble contour in the first step and in the second step the tracking of the bubbles is done by the computer instead of the user. The main problems of this method were

- the varying light reflection on the variable bubble interphase,
- the intensive motions after the coalescence of bubbles,
- the movement of the bubbles out of focus and
- the varying optical characteristics of the background.

The latter is not homogeneous resulting from the surface structure of the heated element which is dark diffuse (sandblasted surface) or strongly reflecting (emery ground surfaces). Additionally, the illumination of the bubbles depends on their local position on the tube (e.g. near the flank of the tube or near the bottom) and it changes with the growth and the movement of the bubbles or by convection effects of the liquid. The total con-

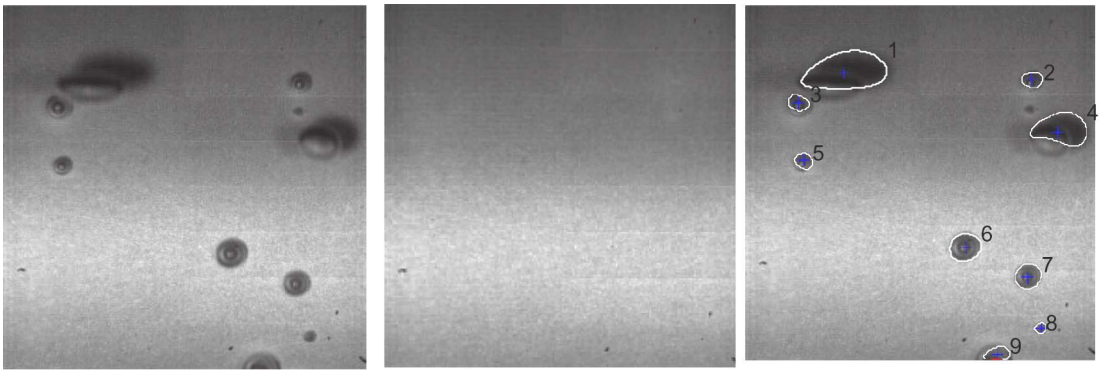

Fig. 4. Example of a single image of a sequence (left), the back ground image (middle) and automatically recognized bubbles 1 to 9, on the right (fine sandblasted copper tube in boiling isopropanol, $p^* = 0.1$ and $q = 3\ \mathrm{kW{\cdot}m^{-2}}$ from [25]).

tour of the bubbles cannot be identified from the background or its shadows by conventional methods for image processing as used for particle image velocimetry (PIV) without prior knowledge of the real shape of the bubble under the specific operating conditions.

In a previous attempt, it was tried to recognize the individual bubbles by so-called "region based snakes" combined with background image identification [25], see Fig. 4. "Region based snake" is a special mathematical procedure of automatic image processing developed for medical application, see [25]. The method aims to detect the contour of the bubbles by analyzing the different grey levels in their surrounding. If the detected contour is interrupted, the contour can be closed by the snake method using the prior knowledge of the bubble form. However, the method is not successful to identify the bubbles even for very low heat fluxes, see Fig. 4, where two bubbles are not recognized and some contours of the bubbles are not correctly described (compare the images in Fig. 4, left and right). The main problem is that the method cannot always separate the bubble shadow from the bubble itself because the image sequence is not considered. It is not possible to track single bubbles correctly on the succeeding images, although the background has been eliminated. Recording the background image without bubbles (for $q \to 0$, i.e. before the heat transfer measurements), see Fig. 4, middle, was not successful either, because the optical property of the superheated liquid and the tube surface change with increasing superheat. Therefore, the background image (Fig. 4, middle) is analysed *by succeeding images in situ* to represent the illuminated surface of the tube immersed within the saturated liquid under the test conditions in the next step of development of a new evaluation method (for the algorithm see [9,25]).

Despite the improvement connected with this modification, the snake technique is limited and cannot track the bubbles on the following images [25]. The further improved semi-automatic method described in this issue [9] is divided into three parts, the bubble identification, the tracking of bubbles and the manual correction if necessary. Because of the last feature, it is semi-automatic again. In the first part the bubbles are determined in a rough approximation. Since the bubble appearance varies according to the test conditions, a database containing various sub-images of typical bubbles for the sequence and the background is established by the user teaching the computer to identify the bubbles in a similar way as the human eye does. Many different sub-images reproduce the various examples of bubbles, but as few as possible should be used to minimize the computation time. Bubbles out of focus are not considered if they have no effect on the bubble formation on the tube and if they are not growing by sliding along the tube, i.e. they are far away from the superheated boundary layer. The user has to determine manually typical shapes of bubbles of certain size by giving four points on the contour of the bubble saved in a second database (see Fig. 5, top). The bubbles can be of circular or elliptic shape. Then, the program starts to track the bubble during its growth and movement along the surface using the template of the bubble appearance and the noted position of the last image. Even the nucleation site can be determined by backtracking of the single bubbles, if its site is located within the area investigated, e.g. No. 42 in Fig. 5.

The entire mathematical procedure for the image processing is described in earlier publications [16,25] and in this special issue [9]. The method is quite robust against the various reflections on the bubble boundary but it is limited to low heat fluxes with some few bubbles and to reduced saturation pressures which are not too low, because nearly circular or elliptic bubble shapes are necessary, nor to high pressures, because then the bubbles are often too small and too numerous and cannot be detected in spite of their more circular shape. All in all, the method still needs relatively high computation capacity.

3. Results for bubble formation

3.1. Review of recently published results

Examples for the result of the evaluation of the video sequences are demonstrated by means of experiments from [3,4, 8] with propane boiling on the outside of a horizontal copper tube with $D = 25.4$ mm and fine sandblasted microstructure. The typical results for the operating parameters are shown in Fig. 6 in form of the heat transfer coefficient α as function of the heat flux q in comparison with the active nucleation sites in Fig. 7. (The video sequences are only investigated for two pressures, see the black symbols in Fig. 6.) The results

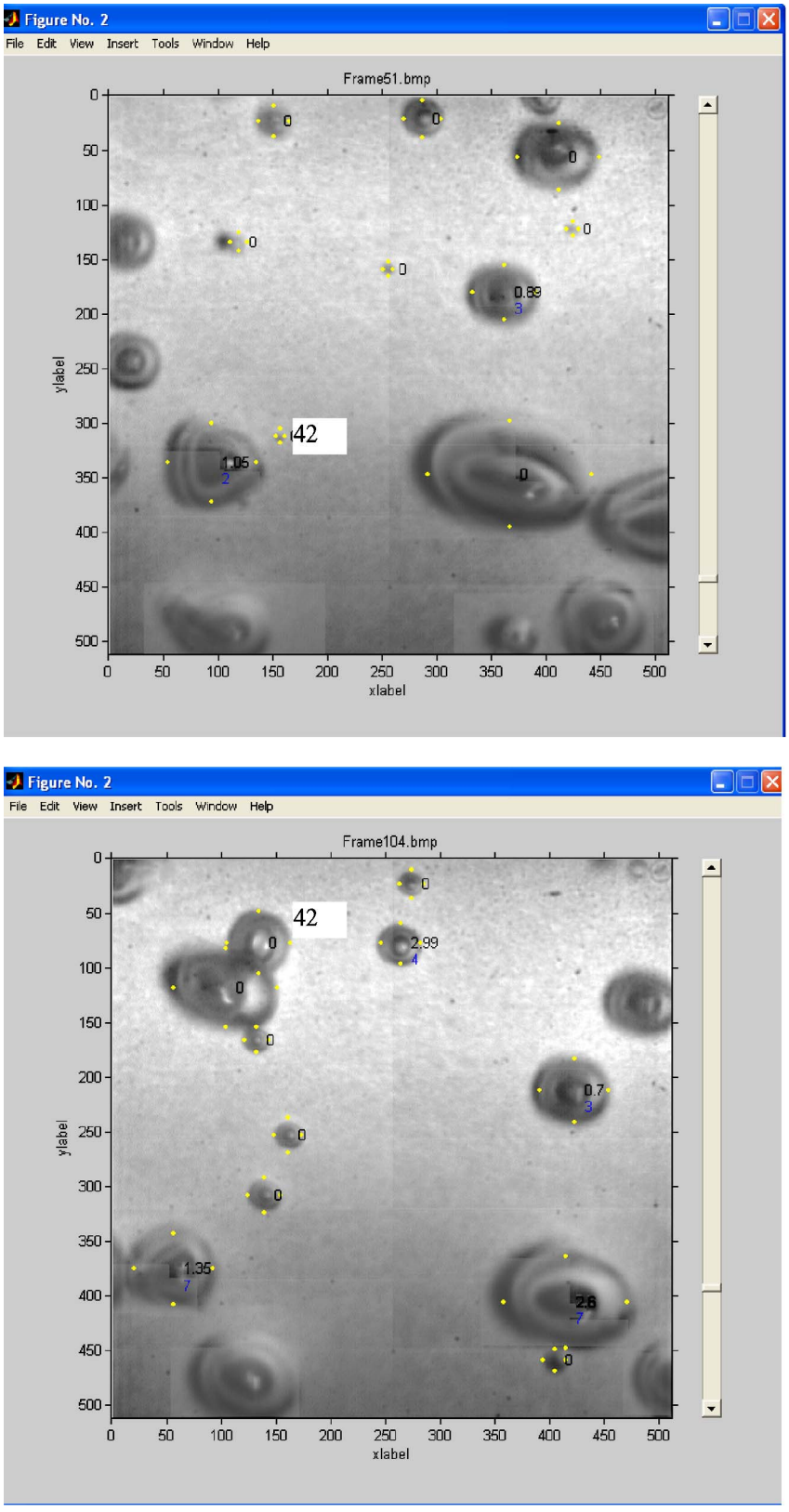

Fig. 5. Bubble formation near the median line of the test tube for propane boiling at $p^* = 0.1$, $q = 5\ \mathrm{kW{\cdot}m^{-2}}$: Tracking of one bubble (No. 42) from its nucleation site (top) to its coalescence with another bubble (bottom).

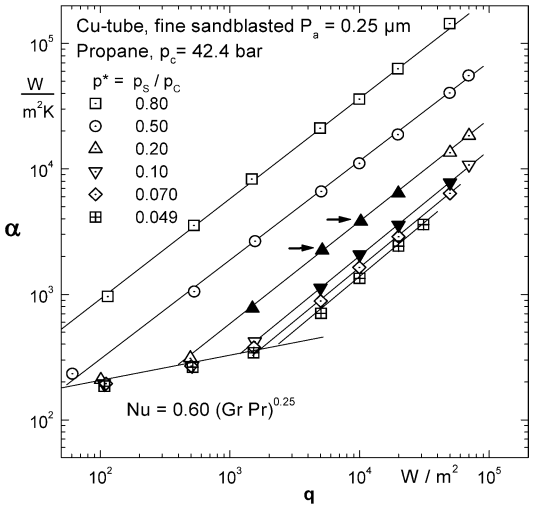

Fig. 6. The heat transfer coefficient α as function of the heat flux q, sandblasted copper tube according to [27,28].

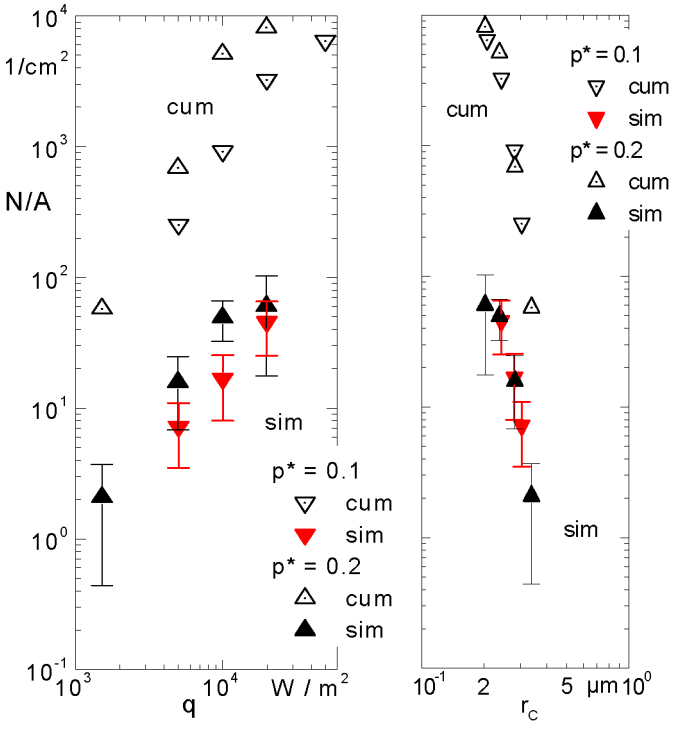

Fig. 7. The number of active sites as function of the heat flux q (left) and of the critical radius r_c of a stable nucleus (right), sandblasted copper tube according to [27,28].

discussed in the following had been obtained by the former, semi-automatic program of [4,15] with permanent input of the user.

The average numbers of cumulative and simultaneous sites for all video sequences investigated for two pressures are shown in Fig. 7 as function of the heat flux (left) and of the critical radius r_c for stable bubble nuclei (right). The critical radius is calculated according to Schömann et al. [26]

$$r_C = \left[\frac{\sigma\rho'}{(\rho'-\rho'')}\right]_{T_W}\left[\frac{T(\rho'-\rho'')}{\Delta h_v \rho'\rho''}\right]_{T_m}\cdot\frac{2}{\Delta T} \qquad (1)$$

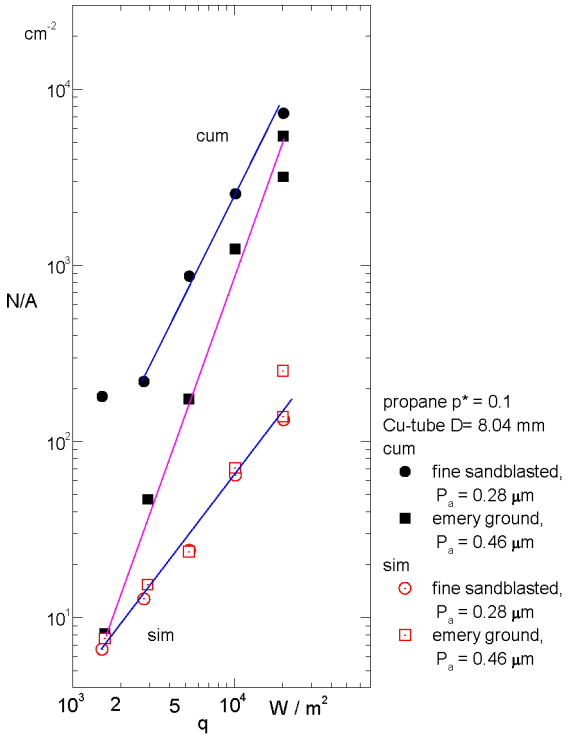

Fig. 8. The number of active sites as function of q for propane boiling on a horizontal copper tube ($D = 8$ mm) with different surface finishes (emery ground and fine sandblasted; from [27,28]).

with the surface tension σ, the density of the saturated liquid ρ' and vapour ρ'' for the wall temperature T_w and the average temperature of the superheated boundary layer $T_m = T_s + \Delta T/2$ and the superheat ΔT. There is a large difference between the cumulative and simultaneous numbers of sites, e.g. the cumulative numbers of sites are 70 times as high as the simultaneous ones for $p^* = 0.2$ and $q = 20$ kW·m^{-2}. The smaller slope for the highest heat fluxes may be due to the difficulty to distinguish properly the single active sites for intensive boiling within the turbulent bubble movement and to the interaction of the growing bubbles with those up-sliding along the heated surface.

Nearly the same heat transfer coefficient α can be related to the same number of mean active simultaneous nucleation sites, e.g. for $p^* = 0.2$ and $q = 10$ kW·m^{-2} and $p^* = 0.1$ and $q = 20$ kW·m^{-2} in Fig. 6 (arrows) and in Fig. 7, right. Similar large potential nucleation sites offered by the surface are obviously activated, because the critical radius calculated with the average superheat has nearly the same value in both cases, see Fig. 7, right. The same holds for the lower heat fluxes $q = 5$ kW·m^{-2} ($p^* = 0.2$) and 10 kW·m^{-2} ($p* = 0.1$). The much higher number of cumulative active sites than those being simultaneously active shows that the same local potential nucleation site is not always activated during the 500 ms. A similarly formed cavity situated just in the nearest neighbourhood is selected for nucleation within the very regular microstructure of the heated surface. The fine sandblasted surface obviously offers a quantity of cavities of similar sizes [3] able to be activated successively in short time.

The number of active sites on other microstructures as e.g. on the axially emery ground surfaces is more stable than on

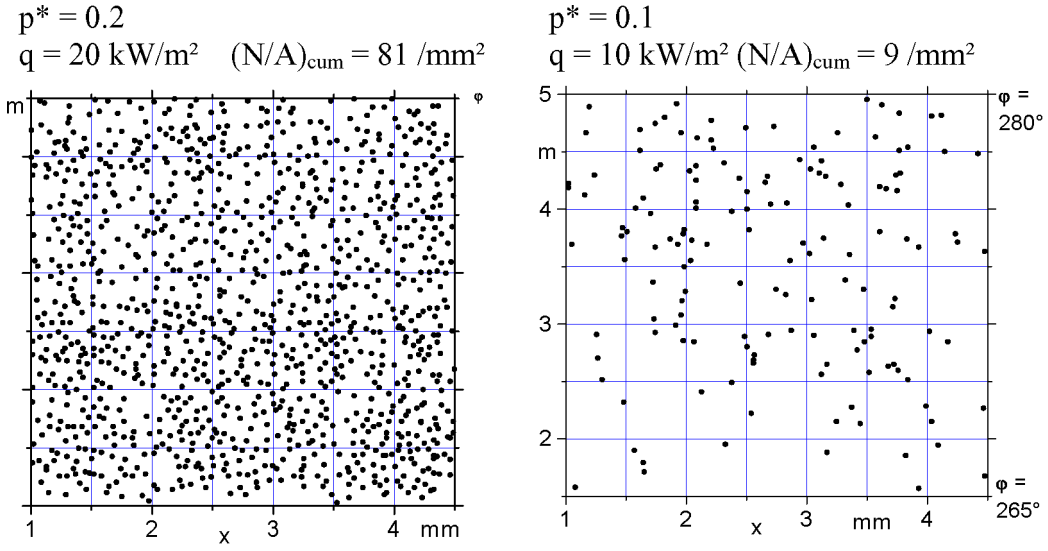

Fig. 9. Local distribution of active cumulative nucleation sites for two heat fluxes and pressures from [27,28].

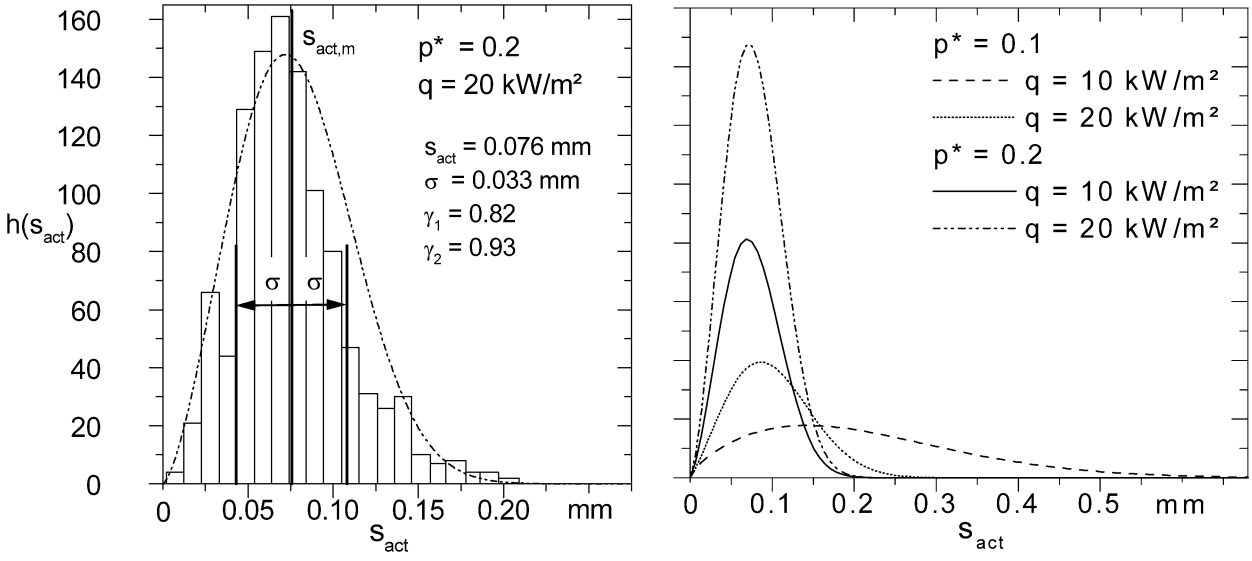

Fig. 10. Distribution of the nearest distances of the active nucleation sites for the high pressure in Fig. 9 as histogram (left), and the Weibull functions (right for different operating conditions) from [27].

the fine sandblasted surface for beginning nucleation, as can be seen by the comparison of the simultaneous and the cumulative sites $(N/A)_k$ in Fig. 8 from [27,28]. The bubbles which are activated in the few large grooves of the emery ground surface analyzed in [3], grow and depart with constant frequency. For higher heat fluxes the differences between simultaneous and cumulative nucleation sites approach those of the fine sandblasted one. For the highest heat flux investigated, the situation is similar to the one on the fine sandblasted surface—a lot of unstable nucleation sites. The number of simultaneous sites on both surfaces is nearly the same, independent of the heat flux. The potential nucleation sites investigated by the analyses of the surface microstructure [3] have to be linked to the active nucleation sites. Therefore, the local distribution on the heated surface is also analysed by means of Figs. 9 and 10.

The local distributions of the cumulative nucleation sites are shown in Fig. 9 for selected operating conditions ($p^* = 0.1$, $q = 10$ kW·m^{-2}, $p^* = 0.2$, $q = 20$ kW·m^{-2}). The angles indicate the azimuthal positions of the sites on the tube (as in Fig. 2). Each area is subdivided in cells for better comparison with the size of the topographies investigated for the roughness analysis [3]. The cumulative site density varies from $(N/A)_{\text{cum}} = 9$ mm^{-2} for $q = 10$ kW·m^{-2} at $p^* = 0.1$ to $(N/A)_{\text{cum}} = 81$ mm^{-2} for $q = 20$ kW·m^{-2} at $p^* = 0.2$. The agglomeration of active sites in the upper part of the tube is remarkable for the lower pressure in Fig. 9, right. This holds particularly for low heat fluxes. The bubbles departing from some few nucleation sites near the bottom of the tube create new active nucleation sites by sliding up the superheated tube surface. The contribution by up-slidinging bubbles is diminished for higher pressures and superheats investigated. The total

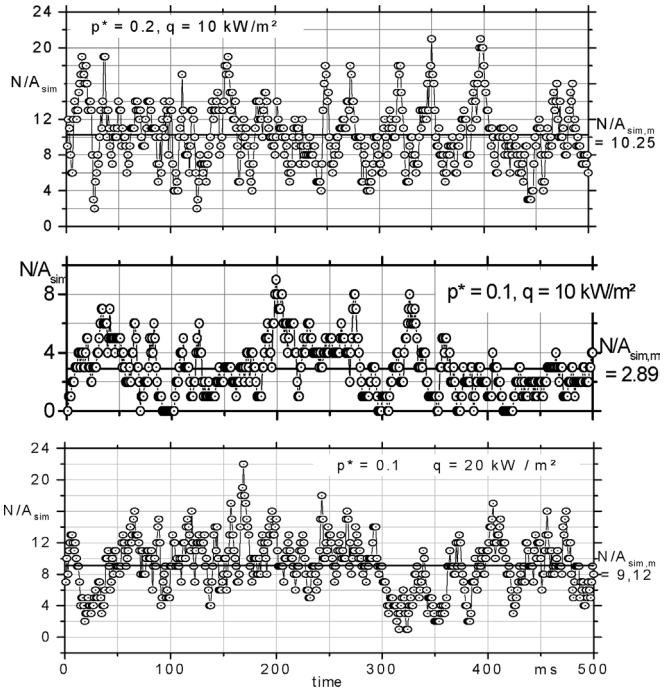

Fig. 11. Temporal resolution of the activation with $(N/A)_{\mathrm{sim}}$ as function of the recording time of the video sequence from [27].

surface of the tube is uniformly covered by active nucleation sites in these cases.

An indication of the interaction between adjacent sites is the statistical analysis of their nearest distances like the distribution in Fig. 10. The histogram for the higher pressure investigated within the area demonstrated in Fig. 9 can be described by a modified Weibull function (see Fig. 10, left) in a similar way as the distribution of the potential sites in [3]. The smallest distances are far away from the value of the critical radius of $r_c = 0.25$ µm, but it is expected that the bubbles will agglomerate during their growth, especially near the departure moment ($d_A \approx 0.15$ mm to 0.25 mm on the flank of the test tube), if they are activated simultaneously. These distributions become wider with decreasing pressure and heat flux. Most often the nearest distance is nearly constant for the two pressures and heat fluxes and can be linked to similar values of the maximum of the distances of the nearest potential sites in [3] for fine sandblasted surfaces.

The number of simultaneous nucleation sites is not constant during the sequence of about 500 images (= 500 ms), see the bars of the standard deviation in Fig. 7. The temporal resolution of the activation is shown in Fig. 11 for some examples. A cycle of activation is succeeded by one of deactivation with a regular fluctuation in the average value of $(N/A)_{\mathrm{sim},m}$. The average value of $(N/A)_{\mathrm{sim},m}$ of the two heat fluxes at two pressures investigated ($q = 10$ kW·m^{-2} at $p^* = 0.2$ and 20 kW·m^{-2} at $p^* = 0.1$) are nearly the same, only the fluctuation seems to be more regular for the higher pressure. The peak-to-valley value $\Delta(N/A)_{\mathrm{sim}}$ increases with pressure and heat flux (from $\Delta(N/A)_{\mathrm{sim}} = 8$ mm^{-2} for $q = 10$ kW·m^{-2} at $p^* = 0.1$ to 16 mm^{-2} at $p^* = 0.2$ and to $\Delta(N/A)_{\mathrm{sim}} = 16$ for $q = 20$ kW·m^{-2} at $p^* = 0.1$, see Fig. 11).

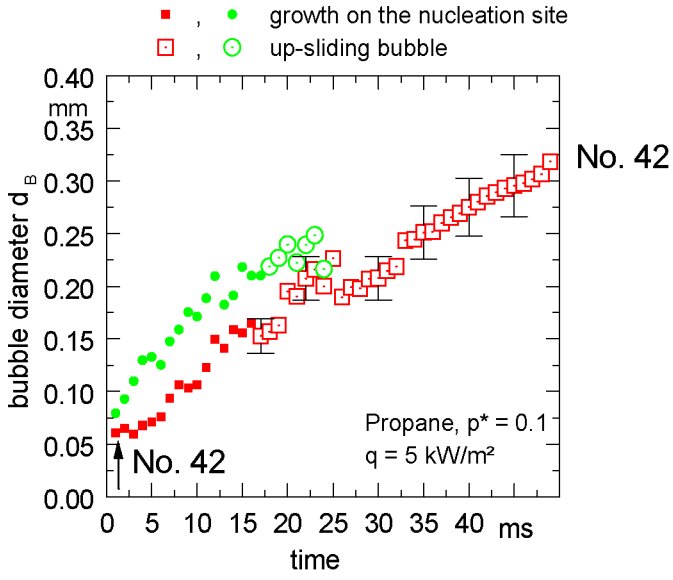

Fig. 12. Two examples of bubbles growing on their nucleation sites and then sliding along the superheated surface.

New coherent results for heat transfer and bubble formation on a horizontal copper tube with different microstructure and macrostructure are discussed in detail by Gorenflo et al. [4] in this special issue, especially dealing with cumulative and simultaneously active nucleation sites on different locations on the tube evaluated with the semi-automatic program [15].

3.2. *New results for bubble growth*

The first results of the evaluation by the new method with the identification and tracking of bubbles of one sequence for propane boiling on a fine sandblasted copper tube surface with $p^* = 0.1$ and a heat flux of $q = 5$ kW·m^{-2} near the median line of the tube is represented in Figs. 12–14. In Fig. 12, bubble No. 42 (from Fig. 5) is identified and tracked until it vanishes from the image (squares). Bubbles smaller than $d_B = 0.05$ mm cannot be detected by this method due to the insufficient resolution in pixels. Shortly after activation the bubble is growing on its nucleation site to the departure diameter ($d_A = 0.16$ mm; closed squares). After departure, it still grows while it is streaming up along the superheated tube surface (open squares). The scatter within the data for the bubble diameter is due to the variation of the visible two-dimensional shape (the projection area) of the bubble, while the third dimension in direction of the tube surface cannot be evaluated. The bubble is only analysed from its top, cf. also Fig. 5. The variation of the shape follows from the influences caused by the movements of the liquid and the up-sliding bubbles. The uncertainties can be estimated to be in the order of 7% to 12% of the values of the bubble diameter. Higher uncertainties have to be considered after the departure of the bubble from its nucleation site, see the error bars in Fig. 12. Steps in two succeeding frames as from 19 to 20 or from 32 to 33 ms show that the bubble has coalesced with second smaller bubble on its site which is located in the way up of the first bubble. After the coalescence, the bubble slides undisturbed along the superheated tube surface and is still growing.

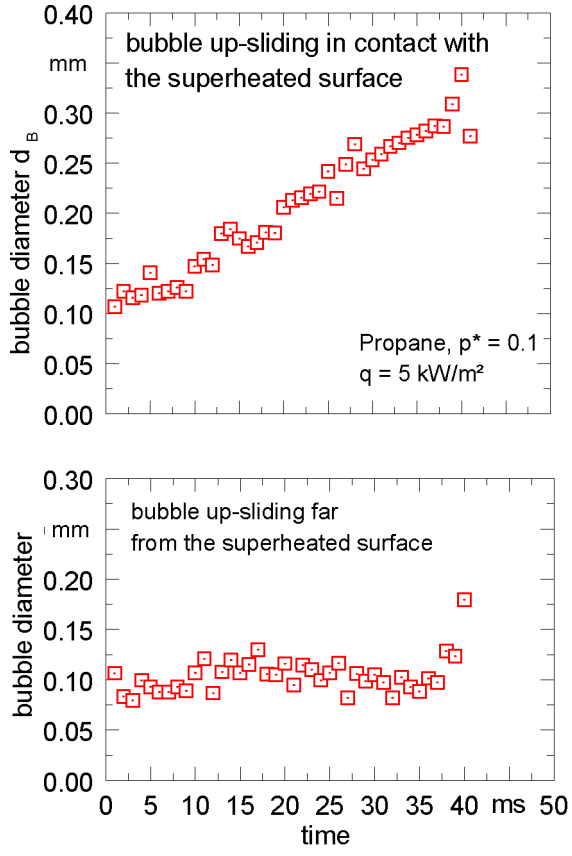

Fig. 13. Examples of bubbles moving upwards and growing (top) or which do not grow (bottom) by sliding along the superheated surface.

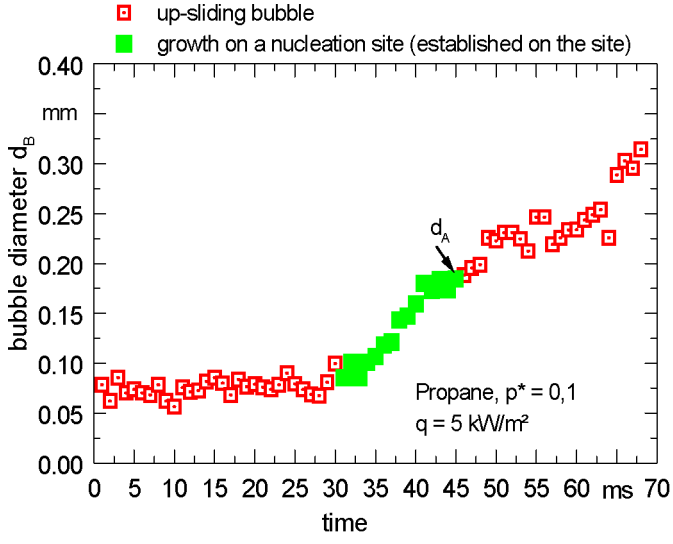

Fig. 14. Example of a bubble sliding upwards, then being established growing on a site and growing further when up-sliding.

The growth of a bubble situated on another nucleation site (circles in Fig. 12) is stronger and it departs with larger diameter from its site ($d_A = 0.21$ mm).

The sliding bubbles can be separated in three types: the first one still grows by contact with the superheated boundary layer during its movement upwards, see Fig. 13, top. The diameter of the second type remains more or less constant because it is obviously far away from the superheated surface. It sudden increase in size results from coalescence with another bubble, see Fig. 13, below. The third type is sliding up close to the superheated surface, then establishes itself on the tube surface (see 30 ms). In the following, it grows there to its departure diameter ($d_A = 0.18$ mm) and remains growing during up-sliding further, see Fig. 14. Other bubbles sliding upwards may create new nucleation sites without visible variation of their shape like type 2, but being somewhat closer to the superheated liquid layer. The nucleation sites activated by up-sliding bubbles are also demonstrated by the activation maps in Figs. 3 and 10 for medium pressures.

The presented data are only some first results of the evaluation of a video sequence. The new method offers the possibility to track single bubbles in video sequences from their activation on the nucleation site to the moment where they leave the heated area investigated. The growth of different bubbles at their nucleation site and during their way sliding up along the superheated boundary layer can be analysed quantitatively and less time consuming as by the former methods.

4. Conclusion

The coherent new data of heat transfer, bubble formation and roughness from the same heated surface gives new idea for the activation of bubbles on the surface, their growth on the site and by sliding up and the manifold interaction between them. The evaluation of high speed video images offers the possibility to receive much more detailed information about the activation of bubbles and of the heated surface and its cavities but it was very time consuming. Semi-automatic and automatic programs are developed to identify and track the individual bubbles. Some video sequences have been analysed previously for a few examples because of the large amount of data. The cumulative active nucleation sites are distributed statistically, especially for low heat fluxes agglomerations are observed over the median line of the horizontal test tube. The density distribution of the nearest distances between the adjacent sites shows that interaction of bubbles growing at their sites is possible if they are active simultaneously. The growth of the bubbles sliding-up along the superheated tube surface results in values nearly twice the bubble departure diameter. Their contribution to the vapour production in model assumptions has to be considered in future. The long-term aim is that the new results shall enable to interpret the fundamentals in boiling heat transfer and to establish new calculation methods using them.

Acknowledgement

The authors highly appreciate financial support of Deutsche Forschungsgemeinschaft (DFG) in the frame of a joint research project on fundamentals of boiling heat transfer. The authors thank all participants of the joint research project for helpful discussions and for their patience.

References

[1] D. Gorenflo, Behältersieden; Abschnitt Hab; VDI-Wärmeatlas, ninth ed., Springer, Berlin, 2002. Cf. also: Pool boiling. Chapt. Ha. VDI-Heat Atlas, VDI-Verlag, Düsseldorf, 1993.

[2] M.G. Cooper, Heat flow rates in saturated nucleate pool boiling—a wide ranging examination using reduced properties, Adv. Heat Transfer 16 (1984) 157–239.

[3] A. Luke, Preparation, measurement and analysis of the microstructure of evaporator surfaces, Int. J. Thermal Sci. 45 (3) (2006) 237–256 (this issue).

[4] S. Kotthoff, D. Gorenflo, E. Danger, A. Luke, Heat transfer and bubble formation in pool boiling: Effect of basic surface modifications for heat transfer enhancement, Int. J. Thermal Sci. 45 (3) (2006) 217–236 (this issue).

[5] E. Hahne, G. Barthau, Heat transfer and nucleation in pool boiling, Int. J. Thermal Sci. 45 (3) (2006) 209–216 (this issue).

[6] M. Buchholz, H. Auracher, T. Lüttich, W. Marquardt, A study of local heat transfer mechanisms along the entire boiling curve by means of microsensors, Int. J. Thermal Sci. 45 (3) (2006) 269–283 (this issue).

[7] P. Genske, K. Stephan, Numerical simulation of heat transfer during growth of single vapor bubbles in nucleate boiling, Int. J. Thermal Sci. 45 (3) (2006) 299–309 (this issue).

[8] D. Gorenflo, W. Fust, A. Luke, E. Danger, U. Chandra, Pool boiling heat transfer from tubes with basic surface modifications for enhancement—Design of the test tubes and first measurements, in: 3rd European Thermal Sci. Conf. Heidelberg, Germany, 2000, vol. 2, pp. 743–748.

[9] D.C. Cheng, H. Burkhardt, Template-based bubble identification and tracking in image sequences, Int. J. Thermal Sci. 45 (3) (2006) 321–330 (this issue).

[10] D. Gorenflo, W. Fath, Heat transfer at pool boiling outside of finned tubes at high saturation pressures, in: Proc. XVIIth Int. Congr. Refrig. Wien 1987, vol. B, pp. 955–960.

[11] P. Genske, K. Stephan, Nucleate boiling—numerical simulation of heat transfer at moderate heat fluxes, in: Proc. Int. Inst. Refrig. Comm. B1 Conf. 2001/5, Paderborn, Germany, 2001, pp. 412–419.

[12] J. Kern, P. Stephan, Assessment of a theoretical model for the nucleate boiling heat transfer coefficient of binary mixtures, in: Proc. 3rd European Thermal Sciences Conference, Heidelberg, Germany, 2000, vol. 2, pp. 779–784.

[13] R.F. Gaertner, Photographic study of nucleate pool boiling on a horizontal surface, J. Heat Transfer (1965) 17–29.

[14] P. Hübner, Gorenflo, A. Luke, Circumferential temperature distributions on plain and finned tubes in pool boiling, in: Proc. 3rd Conf. Compact Heat Exchangers, Davos, Switzerland, 2001, pp. 383–390.

[15] A. Luke, E. Danger, Size distribution of active and potential nucleation sites on horizontal evaporator tubes, in: Proc. Int. Inst. Refrig. Comm. B1 Conf. 2001/5, Paderborn, Germany, 2001, pp. 396–403.

[16] D.C. Cheng, H. Burkhardt, Tracking bubbles in high-speed image sequences, in: Proc. Int. Inst. Refrig., Comm. B1 Conf. 2001/5, Paderborn, Germany, 2001, pp. 388–395.

[17] R. Maurus, V. Ilchenko, T. Sattelmayer, Study of the bubble characteristics and the local void fraction in subcooled flow boiling using digital imaging and analysing techniques, in: Proc. 5th World Conference on Experimental Heat Transfer, Fluid Mechanics and Thermodynamics, Thessaloniki, Greece, 2001, vol. 2, pp. 1329–1336.

[18] F. Mayinger, D. Nordmann, W. Panknin, Holographische Untersuchungen zum unterkühlten Sieden, Chem. Ingenieur Tech. 46 (5) (1974) 209.

[19] D.B.R. Kenning, T. Kono, M. Wienecke, Investigation of boiling heat transfer by liquid crystal thermography, in: Proc. ASME—ZSITS International Thermal Science Seminar, Bled, Slovenia, 2000, pp. 35–46.

[20] M. Buchmann, D. Mewes, Tomographic measurement and reconstruction techniques, in: F. Mayinger (Ed.), Optical measurements—Techniques and Applications, second ed., Springer, Berlin, 1999.

[21] R.F. Gaertner, J.W. Westwater, Population of active sites in nucleate boiling heat transfer, Chem. Engrg. Progr. Sympos. Ser. 56 (1960) 39–48.

[22] M. Weckesser, Untersuchungen zur Blasenbildung beim Sieden in freier Konvektion, Diss., Universität Karlsruhe, TH, 1990.

[23] A. Pinto, D. Gorenflo, W. Künstler, Heat transfer and bubble formation with pool boiling of propane at a horizontal copper tube, in: Proc. 2nd Europ. Therm. Sci. Conf., Rome, Italy, 1996, vol. 2, pp. 1653–1660.

[24] G. Barthau, E. Hahne, Nucleation site density and heat transfer in nucleate pool boiling of refrigerant R134a in a wide pressure range, in: 3rd European Thermal Sci. Conf. Heidelberg, Germany, 2000, vol. 2, pp. 731–736.

[25] D.C. Cheng, H. Burkhardt, Bubble recognition from image sequences, in: Proc. Eurotherm Sem. 68, Poitiers, France, 2001.

[26] H. Schömann, A. Luke, D. Gorenflo, Size distributions of active nucleation sites with pool boiling heat transfer at single tubes with different roughnesses, in: Proc. 10th Int. Heat Transfer Conf., Brighton, UK, 1994, vol. 5, pp. 63–68.

[27] A. Luke, Thermo- und Fluiddynamik beim Sieden—Zusammenhänge zwischen Heizflächenstruktur, Verdampfung und Wärmeübergang, Habilitationsschrift, Universität Paderborn, 2002.

[28] E. Danger, Wärmeübergang und Blasenbildung beim Sieden, Diss., Universität Paderborn, 2004.